J. Physiol. (1964), **171**, *pp.* 302–315
With 13 *text-figures*
Printed in Great Britain

THE ACTION POTENTIAL IN THE MYELINATED NERVE FIBRE OF *XENOPUS LAEVIS* AS COMPUTED ON THE BASIS OF VOLTAGE CLAMP DATA

BY B. FRANKENHAEUSER AND A. F. HUXLEY

From the Nobel Institute for Neurophysiology, Karolinska Institutet, Stockholm 60, *Sweden, and the Department of Physiology, University College London*

(*Received* 28 *October* 1963)

The membrane currents in the myelinated nerve fibre of the toad *Xenopus laevis* have been analysed in previous investigations (Dodge & Frankenhaeuser, 1959; Frankenhaeuser, 1959, 1960, 1962*a*, *b*, *c*, 1963*a*, *b*) with the voltage clamp technique described by Frankenhaeuser & Persson (1957) and Dodge & Frankenhaeuser (1958). For this analysis, membrane potential was changed in steps and membrane current was recorded. Equations were then fitted to the results so as to express the component ionic currents as functions of membrane potential and time. In the present investigation these equations are used to compute the time course of the membrane action potential and of the ionic currents which accompany it, and the results are compared with action potentials recorded from real nerve fibres.

It seems appropriate to sum up some of the findings, and especially some of the uncertainties, of the analysis, before the computations are dealt with.

(1) The membrane currents associated with a potential step are treated as the sum of a capacitive current (I_c) and an ionic current (I_i).

(2) The time resolution of the clamp technique is not sufficient for reliable measurements of I_c. In addition, membrane capacitance (C_m) generally increases during the experiments, an effect which clearly has to do with the application of tight petroleum jelly seals (see Dodge & Frankenhaeuser, 1959).

(3) The ionic currents are treated as the sum of a leak current (I_L), an initial current and a complex delayed current.

(4) The leak current has been measured at anodal steps and at the sodium equilibrium potential. Since the instantaneous $I_L - V$ relation seems to be nearly linear, I_L is treated as $I_L = g_L (V - V_L)$ where g_L is a leak conductance, which is independent of potential and time, and V_L is the

equilibrium potential for the ions carrying I_L. It is evident that this treatment is somewhat arbitrary, because g_L increases when sodium chloride or potassium chloride is added to the ordinary Ringer's solution. This indicates that I_L is carried by both Na^+ and K^+. Further, g_L increases somewhat after cathodal steps of long duration, which is an indication that g_L, is, to some extent, potential- and time-dependent. This is neglected in the analysis.

(5) The initial current has been shown to be carried mainly by sodium ions (Dodge & Frankenhaeuser, 1959) but the initial permeability change is not entirely specific for sodium (Frankenhaeuser & Moore, 1963).

(6) A large part of the complex delayed current has been shown to be carried by potassium (Frankenhaeuser, 1962*a*, *b*, *c*). The potassium permeability change is affected to some extent by choline and sodium on the outside of the membrane. It has not been possible to test how specific the potassium permeability mechanism is.

(7) Some of the complex delayed current was separated as a 'non-specific current' (I_p). This is to a large extent carried by sodium but possibly also by other ions such as calcium (Frankenhaeuser, 1963*a*).

(8) Measurements of instantaneous sodium and potassium currents indicate that the permeability mechanisms which carry these currents show a concentration-dependent rectification of the type described by the 'constant-field equation' (see Behn, 1897; Goldman, 1943; Hodgkin & Katz, 1949; Teorell, 1949; Ussing, 1949; Dodge & Frankenhaeuser, 1959; Frankenhaeuser, 1962*a*, *b*, *c*). The same kind of concentration-dependent rectification can be derived for any permeability mechanism, provided that it has no rectification when concentrations on both sides of the membrane are the same and provided that the independence principle is applicable to the mechanism. The constant-field equation has been used as a convenient approximation for I_{Na} and I_K, the measured rectification of the instantaneous currents and the concentration-dependence of this rectification being the justification for this treatment (Dodge & Frankenhaeuser, 1959; Frankenhaeuser, 1962*c*). The constant-field equation has also been used for I_p, in this case mainly for consistency with I_{Na} and I_K because experimental resolution of the instantaneous $I_p - V$ relation has not been sufficient to decide between the appropriateness of this and other treatments.

(9) The potassium-carrying mechanism shows another type of rectification at very large values of V (Frankenhaeuser, 1962*c*). This rectification is concentration-independent, variable from experiment to experiment, appears at potentials outside the range of normal action potentials and is neglected in the equations describing the voltage clamp data.

(10) I_{Na}, I_K and I_p have been analysed in terms of specific permeabilities P_{Na}, P_K and P_p. These alter as functions of membrane potential and time, but their rates of change are finite even when membrane potential undergoes a step change.

(11) The changes of the permeabilities have been described by equations (4)–(14) below (Frankenhaeuser, 1960, 1963*a*), which were adapted from those used by Hodgkin & Huxley (1952*d*) for the squid giant axon. These express the permeabilities in terms of permeability constants ($\bar{P}_{Na}$, P'_K and $\bar{P}_p$) and variables m, h, n and p; the latter vary with rate constants (α's and β's) which are functions of membrane potential but not of time.

(12) The significance of the absolute values of the permeability constants depends clearly on whether the permeability mechanism is such that the constant-field equation treatment is correct.

(13) The significance of the variables m, h, n and p and the rate constants (α's and β's) is uncertain, but this form of treatment is justified by the fact that the treatment gives a reasonable approximation of a very extensive amount of experimental quantitative data in a relatively simple and compressed form (see Hodgkin & Huxley, 1952*a–d*; Hodgkin, Huxley & Katz, 1952).

(14) The major uncertainties in the work have been the apparent change in membrane capacitance (Dodge & Frankenhaeuser, 1959), the attenuation artifact in the potential recording system (Dodge & Frankenhaeuser, 1958), and the size of the nodal surface area, which is required for calibration of current density.

(15) It has not been possible to carry out a complete analysis on one single fibre; different parts of the data refer to different fibres.

Nomenclature and symbols

Membrane potentials are given as axis-cylinder potential minus outside potential. Outward membrane current is consequently positive. E is used for absolute values of membrane potentials; V is used for potentials relative to resting potential (E_r), thus $V = E - E_r$.

$[Na]_o$; $[Na]_i$	outside and inside sodium concentration	G	membrane conductance
$[K]_o$; $[K]_i$	outside and inside potassium concentration	P_{Na}	sodium permeability
I_{Na}	sodium current	P_K	potassium permeability
I_K	potassium current	P_p	non-specific permeability
I_p	non-specific delayed current	$\bar{P}_{Na}$	sodium permeability constant
I_L	leak current	P'_K	potassium permeability constant
I_c	capacity current	$\bar{P}_p$	non-specific permeability constant
I_i	ionic current		

g_L	leak conductance	m	variable for sodium permeability
C_m	membrane capacitance		
V_{Na}; E_{Na}	sodium equilibrium potential	h	variable for inactivation of sodium permeability
V_K; E_K	potassium equilibrium potential	n	variable for potassium permeability
V_p; E_p	non-specific current equilibrium potential	p	variable for non-specific permeability
V_L; E_L	leak current equilibrium potential	α; β	rate constants for m, h, n and p as indicated by suffix
R	gas constant		
T	absolute temperature	A; B; C	empirical constants in equations for α's and β's
F	Faraday's constant		

Equation system to be computed

This paper deals with the computation of the membrane currents and with the change in membrane potential during the course of a membrane action potential. A membrane action potential is defined as the action potential in a situation where a limited region of membrane is activated uniformly, while current spread to neighbouring regions of the fibre is prevented, i.e. the impulse is local and not conducted.

The simultaneous equations which have to be solved are:

$$I = I_i + I_c, \tag{1}$$

where

$$I_i = I_{Na} + I_K + I_p + I_L, \tag{2}$$

$$I_{Na} = P_{Na}\frac{EF^2}{RT}\frac{[Na]_o - [Na]_i \exp\{EF/RT\}}{1-\exp\{EF/RT\}}. \tag{3}$$

I_p and I_K are computed from similar equations with appropriate concentrations and permeabilities.

$$P_{Na} = \bar{P}_{Na} h m^2, \tag{4}$$

where

$$dm/dt = \alpha_m(1-m) - \beta_m m, \tag{5}$$

and

$$dh/dt = \alpha_h(1-h) - \beta_h h. \tag{6}$$

$$P_p = \bar{P}_p p^2, \tag{7}$$

where

$$dp/dt = \alpha_p(1-p) - \beta_p p. \tag{8}$$

$$P_K = P'_K n^2, \tag{9}$$

where

$$dn/dt = \alpha_n(1-n) - \beta_n n. \tag{10}$$

The values of α's and β's at a potential V are given by the following equations, with the values for the A, B and C given in the data list:

$$\alpha_h = A(B-V)/\{1-\exp((V-B)/C)\}, \tag{11}$$

$$\beta_h = A/\{1+\exp((B-V)/C)\}, \tag{12}$$

$$\alpha_m = A(V-B)/\{1-\exp((B-V)/C)\}, \tag{13}$$

$$\beta_m = A(B-V)/\{1-\exp((V-B)/C)\}. \tag{14}$$

α_p and α_n are given by equations similar to (13) and β_p and β_n by equations similar to (14).

$$I_L = g_L(V-V_L), \tag{15}$$

$$I_c = I-(I_{Na}+I_K+I_p+I_L), \tag{16}$$

$$dV/dt = I_c/C_m. \tag{17}$$

Methods of computation

The computations were made with automatic digital computers, Mercury (University of London Computer Unit) and Wegematic (Computor Division, Karolinska Institutet, Stockholm). The integration method for Mercury was a modified Heun–Runge–Kutta method in which two differential quotients and an error term were computed for each step, the modification being made by A.F.H. The integration method for Wegematic was the ordinary Runge–Kutta method of the fourth order (e.g. Hamming, 1962). Both integration methods are approximations so that they gave slightly different numerical values; the plots differed, however, by not more than the line width in the figures below.

Data list for computations

The equations and the quantitative data obtained in the voltage clamp analysis must to a large extent be considered as approximations. A fair amount of scatter appears especially between values from different fibres. The equation system is so involved that it is impossible in most cases to get even a fair idea of the effect of a change of a single value without going through a complete computation. A 'Standard data list' was therefore made and in order to obtain information about the effect of variations from this 'Standard data' simple changes were made and computations were then performed. When reference is made to such modified data lists then the modifications only are mentioned, indicating that other variables have their standard values.

The initial values at $V = 0$, i.e. the steady-state values at $V = 0$, have to be such that I_i must be zero. The standard data list for I_{Na}, I_K and I_p was made entirely from the experimental data and was not corrected to fulfil this requirement. The value of V_L was adjusted for this purpose. The numerical value of V_L has therefore no other significance than that V remains zero if no external current is applied to the fibre.

Standard data

Table 1 gives the values for A, B and C in the equations (11)–(14).

TABLE 1. Values of parameters in equations (11)–(14) defining the α's and β's

	A ($msec^{-1}$)	B (mV)	C (mV)	Reference
α_h	0·1*	−10*	6*	Frankenhaeuser, 1960
β_h	4·5	+45	10	Frankenhaeuser, 1963*b*
α_m	0·36	+22	3	Frankenhaeuser, 1960
β_m	0·4	+13	20	
α_p	0·006	+40	10	Frankenhaeuser, 1963*a*
β_p	0·09	−25	20	
α_n	0·02	+35	10	
β_n	0·05	+10	10	

* Values modified to give a single curve for experimental results given in Fig. 4 in the paper (Frankenhaeuser, 1960).

$[Na]_o = 114{\cdot}5$ mM $\quad E_r = -70$ mV $\quad \bar{P}_{Na} = 8 \times 10^{-3}$ cm/sec

$[K]_o = 2{\cdot}5$ mM $\quad g_L = 30{\cdot}3$ mmho/cm^2 $\quad \bar{P}_p = 0{\cdot}54 \times 10^{-3}$ cm/sec

$[Na]_i = 13{\cdot}74$ mM $\quad V_L = 0{\cdot}026$ mV $\quad P'_K = 1{\cdot}2 \times 10^{-3}$ cm/sec

$[K]_i = 120$ mM $\quad C_m = 2\ \mu$F/cm^2

Standard initial values: $V = 0$ mV; $h_0 = 0{\cdot}8249$; $m_0 = 0{\cdot}0005$; $p_0 = 0{\cdot}0049$; $n_0 = 0{\cdot}0268$.

RESULTS

An action potential computed with the standard data is shown in Fig. 1, and in Fig. 2 are shown tracings of recorded action potentials to the same scale. The shape of the recorded action potential varied to some extent

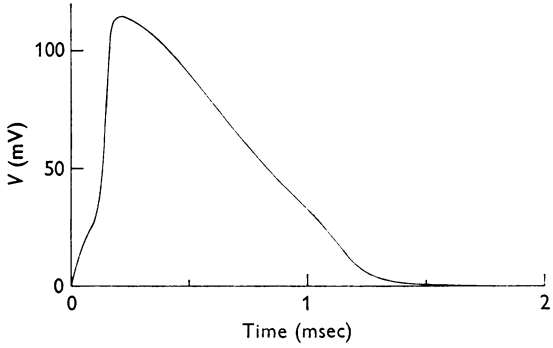

Fig. 1. Computed action potential. Standard data. Stimulating current $I =$ 1 mA/cm^2 when $0 < x < 0{\cdot}12$ msec and $I = 0$ when $x > 0{\cdot}12$ msec.

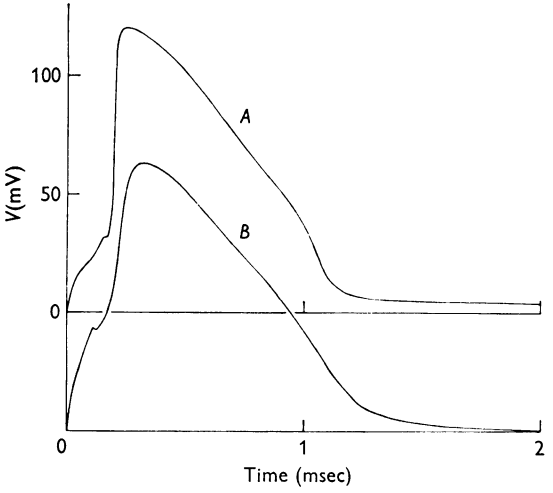

Fig. 2. Recorded action potentials from two axons. Ordinates for *B* shifted 50 mV down. Temperature 20° C. Axon in *A* polarized continuously with a weak anodal current in order to show the slowly decaying after-potential in this situation.

from fibre to fibre. The general agreement between the computed action potential and the recorded potentials seems satisfactory in spite of minor deviations.

Figure 3 shows how the variables h, m, n and p change during the 'standard' action potential and Fig. 4 shows the calculated permeability changes. The calculated membrane conductance (G) during the action potential is plotted in Fig. 5 and the ionic currents are shown in Fig. 6.

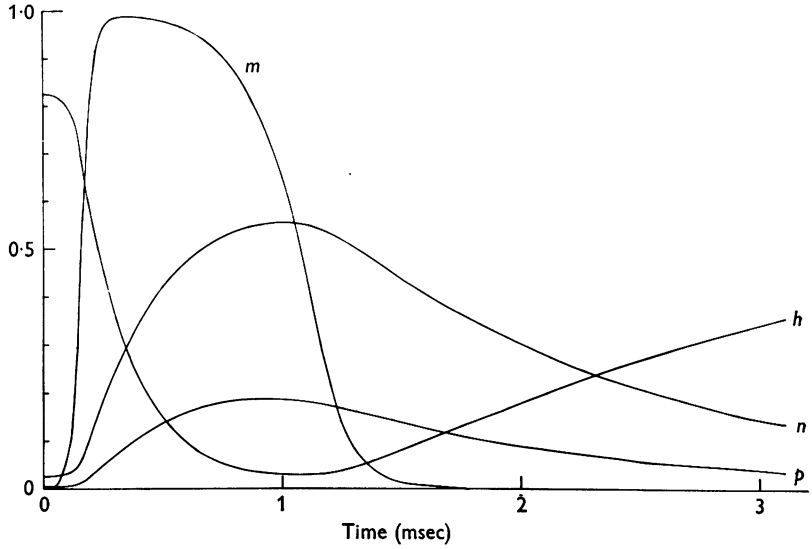

Fig. 3. Computed variables h, m, n and p during action potential (Fig. 1), standard data.

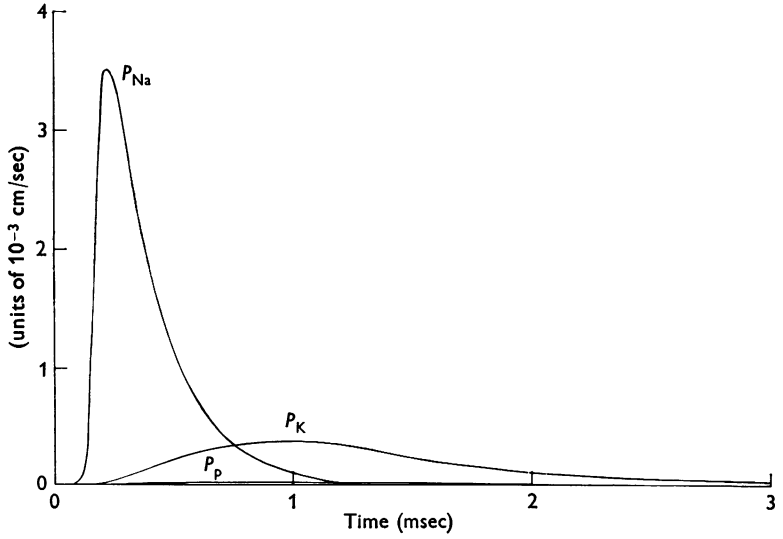

Fig. 4. Computed P_{Na}, P_K and P_p during action potential (Fig. 1); standard data.

The computed as well as the recorded action potentials were followed by only a negligible after-potential, in spite of the fact that the permeability changes were far from their resting values at the end of the action potential. The variables h, m, n and p, and the permeabilities P_{Na}, P_K and P_p, each went through a single peaked change and so did G, I_K and I_p. I_{Na},

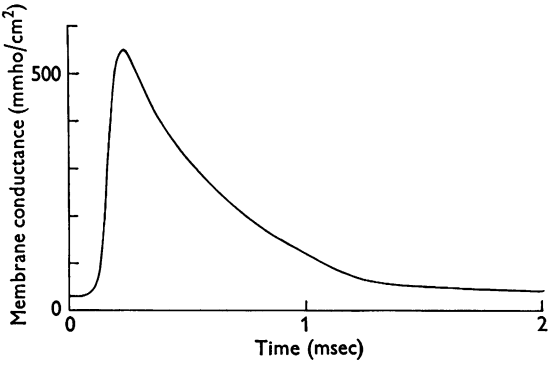

Fig. 5. Computed membrane conductance (G) during action potential (Fig. 1); standard data.

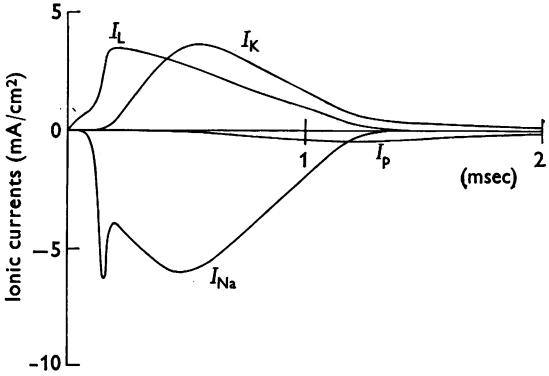

Fig. 6. Computed I_{Na}, I_K, I_p and I_L during action potential (Fig. 1); standard data. Nodal area 120×10^{-8} cm².

however, had two peaks, one just before and one just after the peak of the action potential. This agrees well with the corresponding findings for the squid fibre (Hodgkin & Huxley, 1952*d*).

The experimental analysis indicated a fair amount of scatter both in the permeability constants and in the rate constants. It was therefore decided to compute action potentials with some rather extreme changes in these constants, in order to obtain some idea of how much the action potential is affected by various modifications. The equation system is too

complicated to make simple approximations profitable, since all the currents are as a rule affected by a change of a single value in the data list.

The maximum sodium current in the voltage clamp experiments was from -30 to -40 mA/cm^2, while in the action potential it was only

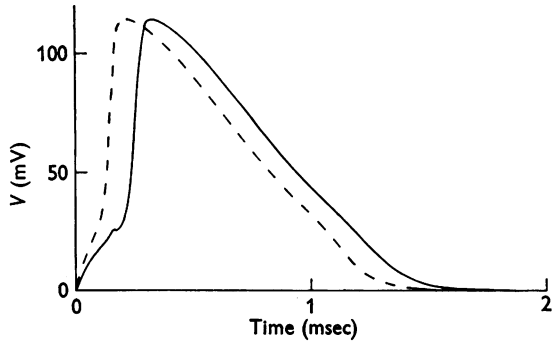

Fig. 7. Computed action potential. $C_m = 4$ μF/cm^2, otherwise standard data. $I = 1$ mA/cm^2 when $0 < x < 0{\cdot}16$ msec; $I = 0$ when $x > 0{\cdot}16$ msec. Interrupted line computed with standard data.

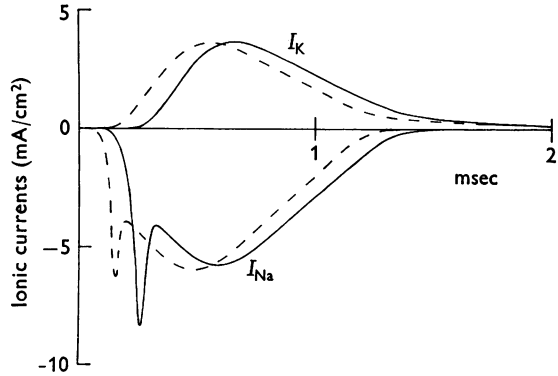

Fig. 8. Computed I_{Na} and I_K during action potential (Fig. 7). $C_m = 4$ μF/cm^2. Interrupted lines computed with standard data.

$-6{\cdot}3$ mA/cm^2. This finding might indicate that the membrane can be loaded considerably without too obvious a change in the action potential. An action potential was computed with the standard data, except the value of C_m which was increased from 2 μF/cm^2 to 4 μF/cm^2. Figure 7 shows the computed action potential, while Fig. 8 shows the corresponding I_{Na} and I_K. The initial part of the action potential, during which the membrane was still nearly passive, was clearly slower. The other parts of the action potential were, however, only little affected. The maximum rate of rise

was 1904 V/sec in the standard action potential while it was 1483 V/sec with the increased value of C_m. The peak of the action potential was 114·6 mV when C_m was 2 μF/cm^2 and 113·9 mV when C_m was 4 μF/cm^2. The first peak in the sodium current increased from $-6{\cdot}3$ to $-8{\cdot}3$ mA/cm^2 (Fig. 8), while the second peak changed only little, from $-6{\cdot}0$ to $-5{\cdot}8$ mA/cm^2.

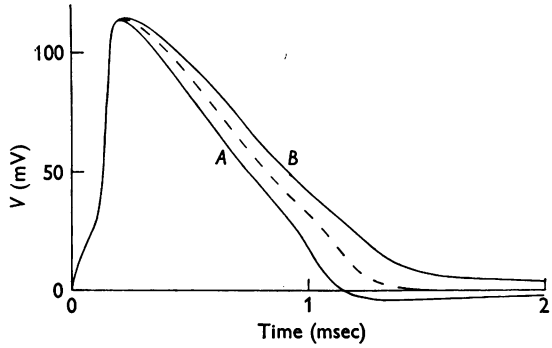

Fig. 9. Computed action potential. $P'_K = 2{\cdot}4 \times 10^{-3}$ cm/sec in A; $P'_K = 0{\cdot}6 \times 10^{-3}$ cm/sec in B; otherwise standard data. Interrupted line computed with standard data.

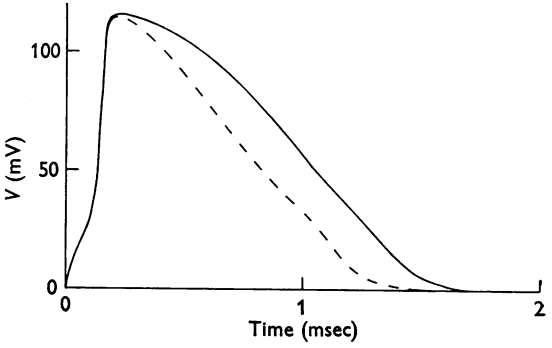

Fig. 10. Computed action potential. $P'_K = 0$ and $\bar{P}_p = 0$; otherwise standard data. Interrupted line computed with standard data.

The potassium permeability change varied considerably in the experimental data. Computations were therefore made where P'_K was changed. In Fig. 9 A and B it was $2{\cdot}4 \times 10^{-3}$ and $0{\cdot}6 \times 10^{-3}$ cm/sec respectively, instead of the standard value $1{\cdot}2 \times 10^{-3}$ cm/sec, while P'_K and $\bar{P}_p$ were zero in Figs. 10 and 11. It is clear that a moderate change of the potassium permeability mechanism has only a small effect on the action potential, and that it mainly affects the falling phase of the action potential and the after-potential. The second peak in the sodium current disappeared

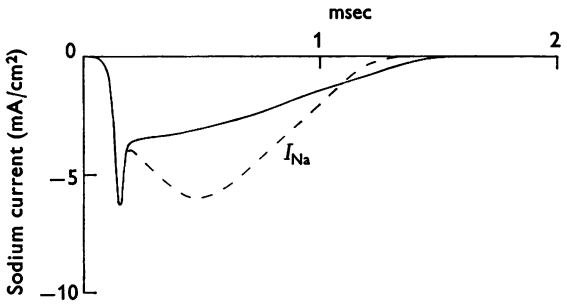

Fig. 11. Computed I_{Na} during action potential (Fig. 10). $P'_K = 0$ and $\bar{P}_p = 0$. Interrupted line computed with standard data.

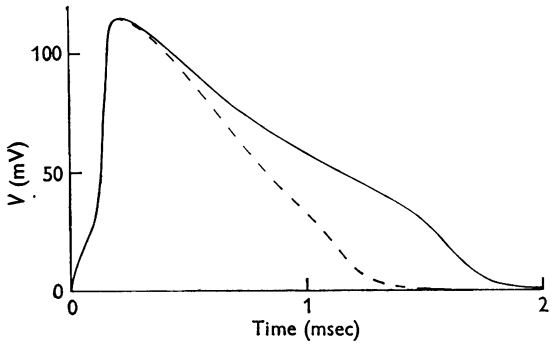

Fig. 12. Computed action potential. $\beta_h = 0{\cdot}05(V-32)/\{1-\exp(32-V)/10\}$; otherwise standard data. Interrupted line computed with standard data.

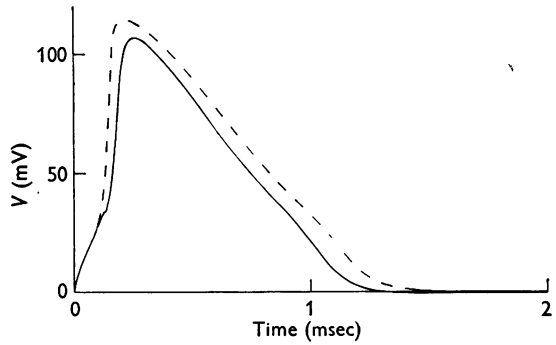

Fig. 13. Computed action potential. $\bar{P}_{Na} = 4 \times 10^{-3}$ cm/sec; otherwise standard data. Interrupted line computed with standard data.

when P'_K was zero and increased considerably when P'_K was $2{\cdot}4 \times 10^{-3}$ cm/sec, being $-7{\cdot}83$ mA/cm^2 instead of $-5{\cdot}98$ mA/cm^2.

The time course of the sodium inactivation was complicated (see

Frankenhaeuser, 1963); some computations were therefore made where β_h was varied. Figure 12 is computed with the original equation for β_h (see Frankenhaeuser, 1959) and it is seen that the duration of the action potential was considerably prolonged.

A computation was also made where the value of $\bar{P}_{Na}$ was decreased from 8×10^{-3} to 4×10^{-3} cm/sec (Fig. 13) and it was noted that the changes in the action potential were relatively small for such a considerable change: the peak of the action potential was 106·6 instead of 114·6 mV and the maximum rate of rise decreased to 1264 V/sec.

DISCUSSION

This paper deals with the computation of the membrane action potential in the myelinated nerve fibre on the basis of the voltage clamp analysis made earlier. The computed action potential agreed reasonably well with recorded action potentials. Deviations were noted but these were not larger than what would be expected from the scatter and from the uncertainties in the experimental data. It seems therefore safe to conclude that this voltage clamp treatment gives a fair description of the currents in the myelinated fibre, and there seems to be no requirement for other currents of substantial magnitude for the understanding of the impulse activity in the myelinated fibre. The permeability relations in the resting fibre have not yet been sufficiently investigated to be quantitatively accounted for in this treatment (see Schmidt & Stämpfli, 1959; Stämpfli, 1959). These are somewhat arbitrarily grouped together in the terms I_L, g_L and V_L. This treatment covers only the 'normal' nerve fibre. Action potentials from fibres in abnormal conditions, for example in solutions with tetraethylammonium or nickel (Tasaki, 1959), can be considered only when sufficient voltage clamp data are available (see Dodge, 1961).

The main aim with which the voltage clamp experiments on single nodes of Ranvier were undertaken was to increase our understanding of the permeability mechanism by obtaining a resolution sufficient to detect permeability changes at single permeability sites. It has not been possible to achieve this resolution. The mechanism of the permeability changes remains unknown, but the voltage clamp data set rather sharp limits for any hypothesis in this field (see also Hodgkin & Huxley, 1952*d*).

Finally, attention is drawn to the striking similarity between these results on vertebrate fibres and the corresponding results on the squid giant axon (Hodgkin & Huxley, 1952*a–d*; Hodgkin, Huxley & Katz, 1952). The mechanisms of impulse conduction in these very different types of nerve fibre are similar in their main outlines but different in detail in most respects. In both cases the currents are carried mainly by sodium and potassium, and these ions move with their electro-chemical driving

forces, but the rectification properties, the current densities, and the rate constants for the permeability changes, all show substantial differences.

SUMMARY

1. Computations on a digital computer were made from the voltage clamp data obtained earlier in experiments on the myelinated nerve fibre of *Xenopus laevis*.

2. Solutions were obtained for the situation where a membrane action potential was discharged.

3. Graphs are presented showing the calculated: (*a*) action potential; (*b*) permeability variables m, h, n and p; (*c*) permeabilities P_{Na}, P_K and P_p; (*d*) membrane conductance G; (*e*) ionic currents I_{Na}, I_K, I_p and I_L.

4. Computations were further made for simple changes of the voltage-clamp data.

5. The solutions are compared with recorded membrane action potentials.

6. It is concluded that the voltage clamp data predict an action potential which agrees satisfactorily with recorded action potentials. Currents of an appreciable amplitude, others than those described in the voltage clamp analysis, are therefore not required to explain the impulse activity in the myelinated nerve fibre.

This investigation was supported by the Swedish Medical Research Council and Stiftelsen Therese och Johan Anderssons Minne. We wish to express our thanks to the University of London Computer Unit and to the Computor Division at Karolinska Institutet.

REFERENCES

BEHN, U. (1897). Ueber wechelseitige Diffusion von Elektrolyten in verdünnten wässrigen Lösungen, insbesonders über Diffusion gegen das Concentrationsgefälle. *Ann. Phys., Lpz.*, N. F. **62**, 54–67.

DODGE, F. A. (1961). Ionic permeability changes underlying nerve excitation. *Biophysics of Physiological and Pharmacological Actions*, pp. 112–143. Washington: American Association for the Advancement of Science.

DODGE, F. A. & FRANKENHAEUSER, B. (1958). Membrane currents in isolated frog nerve fibre under voltage clamp conditions. *J. Physiol.* **143**, 76–90.

DODGE, F. A. & FRANKENHAEUSER, B. (1959). Sodium currents in the myelinated nerve fibre of *Xenopus laevis* investigated with the voltage clamp technique. *J. Physiol.* **148**, 188–200.

FRANKENHAEUSER, B. (1959). Steady state inactivation of sodium permeability in myelinated nerve fibres of *Xenopus laevis*. *J. Physiol.* **148**, 671–676.

FRANKENHAEUSER, B. (1960). Quantitative description of sodium currents in myelinated nerve fibres of *Xenopus laevis*. *J. Physiol.* **151**, 491–501.

FRANKENHAEUSER, B. (1962*a*). Delayed currents in myelinated nerve fibres of *Xenopus laevis* investigated with voltage clamp technique. *J. Physiol.* **160**, 40–45.

FRANKENHAEUSER, B. (1962*b*). Instantaneous potassium currents in myelinated nerve fibres of *Xenopus laevis*. *J. Physiol.* **160**, 46–53.

FRANKENHAEUSER, B. (1962*c*). Potassium permeability in myelinated nerve fibres of *Xenopus laevis*. *J. Physiol.* **160**, 54–61.

FRANKENHAEUSER, B. (1963*a*). A quantitative description of potassium currents in myelinated nerve fibres of *Xenopus laevis*. *J. Physiol.* **169**, 424–430.

FRANKENHAEUSER, B. (1963*b*). Inactivation of the sodium-carrying mechanism in myelinated nerve fibres of *Xenopus laevis*. *J. Physiol.* **169**, 445–451.

FRANKENHAEUSER, B. & MOORE, L. E. (1963). The specificity of the initial current in myelinated nerve fibres of *Xenopus laevis*. Voltage clamp experiments. *J. Physiol.* **169**, 438–444.

FRANKENHAEUSER, B. & PERSSON, A. (1957). Voltage clamp experiments on the myelinated nerve fibre. *Acta physiol. scand.* **42**, Suppl. 145, 45.

GOLDMAN, D. E. (1943). Potential, impedance, and rectification in membranes. *J. gen. Physiol.* **27**, 37–60.

HAMMING, R. W. (1962). *Numerical Methods for Scientists and Engineers*, p. 212. London: McGraw-Hill Book Company, Inc.

HODGKIN, A. L. & HUXLEY, A. F. (1952*a*). Currents carried by sodium and potassium ions through the membrane of the giant axon of *Loligo*. *J. Physiol.* **116**, 449–472.

HODGKIN, A. L. & HUXLEY, A. F. (1952*b*). The components of membrane conductance in the giant axon of *Loligo*. *J. Physiol.* **116**, 473–496.

HODGKIN, A. L. & HUXLEY, A. F. (1952*c*). The dual effect of membrane potential on sodium conductance in the giant axon of *Loligo*. *J. Physiol.* **116**, 497–506.

HODGKIN, A. L. & HUXLEY, A. F. (1952*d*). A quantitative description of membrane current and its application to conduction and excitation in nerve. *J. Physiol.* **117**, 500–544.

HODGKIN, A. L., HUXLEY, A. F. & KATZ, B. (1952). Measurement of current-voltage relations in the membrane of the giant axon of *Loligo*. *J. Physiol.* **116**, 424–448.

HODGKIN, A. L. & KATZ, B. (1949). The effect of sodium ions on the electrical activity of the giant axon of the squid. *J. Physiol.* **108**, 37–77.

SCHMIDT, H. & STÄMPFLI, R. (1959). Das Ruhepotential markhaltiger Nervenfasern in natrium- und chlorarmen Ringer-Lösungen. *Helv. physiol. acta*, **17**, 62–81.

STÄMPFLI, R. (1959). Is the resting potential of Ranvier nodes a potassium potential? *Ann. N. Y. Acad. Sci.* **81**, 265–284.

TASAKI, I. (1959). Demonstration of two stable states of the nerve membrane in potassium-rich media. *J. Physiol.* **148**, 306–331.

TEORELL, T. (1949). Membrane electrophoresis in relation to bio-electrical polarization effects. *Arch. Sci. physiol.* **3**, 205–219.

USSING, H. H. (1949). The distinction by means of tracers between active transport and diffusion. *Acta physiol. scand.* **19**, 43–56.